

Electronic structure of the Pt(001) surface with and without an adsorbed gold monolayer

Ding-sheng Wang

Department of Physics, Northwestern University, Evanston, Illinois 60201

A. J. Freeman

*Department of Physics, Northwestern University, Evanston, Illinois 60201
and Argonne National Laboratory, Argonne, Illinois 60439*

H. Krakauer

Department of Physics, College of William and Mary, Williamsburg, Virginia 23185

(Received 15 August 1983)

Results of all-electron self-consistent semirelativistic local-density-functional linearized-augmented-plane-wave (LAPW) investigations of the clean and Au-covered Pt(001) surface are presented. The charge density within the fourfold hollow sites at the surface was found to be very similar on both surfaces, as expected. The work function of the Au/Pt surface was reduced by 0.43 eV compared to the clean Pt surface. The interface atom $4f_{7.2}$ core-state level on the Au/Pt surface is shifted by 0.3 eV to reduced binding energy. On the clean Pt surface, the density of states (DOS) on the surface atomic layer shows a large peak at about -1.0 eV due to surface states. This peak persists at -1.0 eV after Au coverage on the Au/Pt surface and is due to a band of interface states localized on the interface Pt atomic layer. Significantly, however, there are *no* states on the Au/Pt surface which are localized both on the Au and interface-Pt layers. Furthermore, the *d*-band DOS on the adsorbed Au layer is fully occupied. These results are used to discuss the experimentally observed enhanced reactivity of the Au/Pt surface and lead to the conclusion that the morphology of the experimentally observed surface may be quite different from that previously thought and modeled here.

I. INTRODUCTION

One of the most tantalizing prospects in surface science is that experimental and theoretical studies of well-characterized single-crystal surfaces may significantly advance our basic understanding of the fundamental processes involved in heterogeneous catalysis.¹⁻³ This hope has been intensified as a result of dramatic advances in theoretical methods and experimental techniques in the last decade. By contrast with commercial highly dispersed catalysts,¹ where it is very difficult to separate structural from compositional effects,²⁻⁷ studies of reactions on well-defined single-crystal surfaces⁸⁻¹⁸ have the advantage of allowing independent control of these effects, since these quantities can be directly monitored using a rapidly increasing number of powerful experimental surface techniques such as low-energy electron diffraction (LEED), Auger spectroscopy, photoemission, ion scattering, surface extended x-ray-absorption fine structure (SEXAFS), ion-neutralization spectroscopy, and electron and photon-stimulated desorption. Prototypical experimental studies on this type have been carried out by Somorjai and co-workers on single-crystal surfaces of platinum,^{8,10,13,15} an important catalyst in various hydrogenations and dehydrogenations of hydrocarbons, especially in the production of gasoline.¹⁹ By studying surfaces with variable concentrations of step and kink sites (which may be related to structural features whose concentrations vary with the particle size of dispersed com-

mercial catalysts) they were able to demonstrate the importance of such special sites in controlling the activity and selectivity for several catalyzed hydrocarbon reactions.¹³

Recently, these studies were extended¹⁴ to investigate the catalytic activity of alloys^{5,7,15-18} formed from metals in groups VIII and *Ib* in the Periodic Table, where enhanced reaction rates and selectivity have been observed^{5,7,14} upon alloying a chemically active group-VIII metal such as Pt with an inactive group-*Ib* metal such as Au. In this recent study,¹⁴ cyclohexene dehydrogenation (to benzene) rates were enhanced about fivefold relative to the clean Pt(001) surface by a single ordered monolayer of Au on Pt(001) and also by ordered Pt layers on the inactive Au(001) surface. At Au coverages above one monolayer the reaction rates dropped off dramatically. Depositing Pt on Au, they found the dehydrogenation rate to increase with Pt coverage, reaching a maximum 6 times higher than that of clean Pt(001) between one and two Pt overlayers, and the reaction rate retained that value at higher Pt coverages. Because gold itself is chemically inactive, this observation has raised important questions about our present understanding of how the electronic structure of ordered metal overlayers affects both the physical and chemical properties of catalytically active surfaces. Obviously, knowledge of the electronic structure of both the clean and covered surfaces is important for understanding these properties.

The (001) surface of Pt and its neighbors in the Periodic

Table, Ir and Au, are reconstructed at room temperature and characterized by a (5×1) LEED pattern. LEED studies¹⁴ showed that deposition of Au on Pt(001) removed the reconstruction of the clean Pt(001) surface and that deposition of Pt on Au(001) removed the reconstruction of the Au(001) surface, with a (1×1) pattern of sharp spots observed in both cases at monolayer coverages. Measurements of spot-to-spot distances showed that Au assumed the Pt(001)-substrate lattice constant, up to a coverage of two layers, implying a contraction of 4% with respect to the bulk-Au lattice constant. Similar measurements¹⁴ showed that Pt assumes the Au(001)-substrate lattice constant, implying a 4% expansion relative to bulk Pt. In both cases the overlayers seemed to fit in exact registry on top of the substrate.

Although no definite explanation could be given to explain the observed reactivity enhancement for Au deposited on the Pt(001) surface, several possibilities were considered. Deposited Au, as was suggested by Sachtler *et al.*,¹⁴ could block certain sites where the competing carbon-carbon bond-breaking processes (which lead to surface deactivation by carbon deposition) take place, thereby increasing the rate of carbon-hydrogen bond breaking. This was consistent with their observation by Auger spectroscopy that no carbon was deposited on Pt(001) covered by one or more layers of gold. In contrast, half-monolayer carbon coverage was found in the experiment on the clean Pt(001) surface. Noting that the reaction rate reaches a maximum for full coverage at one monolayer of gold, they suggested the possibility of unique bonding of the cyclohexene to the top-layer Pt atoms which are centered just below the fourfold hollow sites in the Au monolayer.²⁰ These Pt atoms are accessible through the relatively open hollows. Finally, since Pt has a higher work function than Au, the resulting charge transfer could significantly influence the bonding of hydrocarbons.

Several possible explanations for enhanced rates of Pt deposited on Au were also discussed.¹⁴ Unlike Au deposited on Pt, where a layer-by-layer growth model was deduced, Pt deposited on Au may be present as crystallites, whose edge atoms could be more active than the Pt atoms on the smooth surface. Charge transfer and other electronic interactions were also considered, as was the possibility that the reactivity of Pt or Au is altered by the 4% lattice expansion of the Pt overlayers.

In this paper, we present results of investigations of the clean Pt(001) surface with and without an ordered Au-monolayer overlayer. The organization of the paper is as follows. In Sec. II we briefly discuss the details of the theoretical method. In Sec. III we present and discuss our results and their relevance to experimental measurements. Finally, in Sec. IV we present our principal conclusions.

II. METHODOLOGY

In our calculation, a five-layer Pt(001) unreconstructed slab covered with an ordered Au monolayer on each side (referred to as Au/Pt) is used to theoretically model the actual surface. The geometry is determined by the bulk Pt crystal (fcc, $a = 7.41$ a.u.), including the distance between

the Au overlayers and the Pt surface. Calculations are also performed on an idealized clean Pt(001) five-layer slab without any reconstruction or relaxation as well as an isolated Au-monolayer film. For the purpose of comparison, the lattice parameter of this isolated Au-monolayer film is set equal to that of the Au/Pt slab (4% contraction with respect to the bulk Au lattice).

Our self-consistent linearized-augmented-plane-wave (LAPW) film method^{21,22} is used with the Hedin-Lundqvist exchange-correlation term.²³ The core charge density is computed self-consistently for every iteration in a fully relativistic Dirac-Slater-type atomic structure program. The valence states are computed semirelativistically, i.e., the Dirac equation is solved including mass-velocity and Darwin terms but without the spin-orbit-coupling-term effects. No shape approximations are made for the potential or charge density in the vacuum and interstitial regions, but the potential is assumed spherically symmetric inside touching muffin-tin spheres (a very good approximation for metals²²).

For the Au/Pt system (seven atoms per unit cell), the basis size of over 190 LAPW's per z -reflection symmetry type (54 LAPW's per atom) results in eigenvalues converged to better than 5 mRy. Ten \vec{k} points in the $\frac{1}{8}$ th irreducible wedge of the two-dimensional (2D) Brillouin zone are used to generate the charge density in the self-consistency process. The degree of self-consistency achieved, as measured by the rms difference between input and output potential, is 14 mRy. For this rms error in the potential, the integrated charge density (and hence charge transfers) in the muffin-tin spheres and vacuum region are converged to better than 0.01 electrons, while the eigenvalues are converged to better than 1 mRy. For the clean Pt(001) five-layer film, 56 LAPW's per atom are used and the self-consistency is 6 mRy. For the isolated Au-monolayer film, where 60 LAPW's per atom are used, self-consistency at the level of 0.7 mRy has been achieved.

III. RESULTS AND DISCUSSION

The total charge density of the Au/Pt and the clean Pt(001) slabs are depicted as contour plots in Fig. 1. These plots are for a vertical plane passing through a face of the cubic conventional unit cell of the fcc crystal. The charge densities in these two slabs are seen to be very similar in the interstitial and vacuum regions.

The charge density is essentially bulklike only one layer away from the surface atomic layer for both slabs. There are no essential changes in the charge density within the fourfold-coordinated hollow site in the surface atomic layer on the Au/Pt compared to the clean Pt slab except, of course, for the fact that Au atoms define the hole on Au/Pt. The differences between the physical and chemical properties of Pt and Au are largely due to difference in d -band occupation. The d charge density is more localized near the atom center, and these regions are left blank in Fig. 1, due to the very large and rapidly varying electron density there.

A more quantitative description of these differences in d -band occupancy is given by Table I, which shows the to-

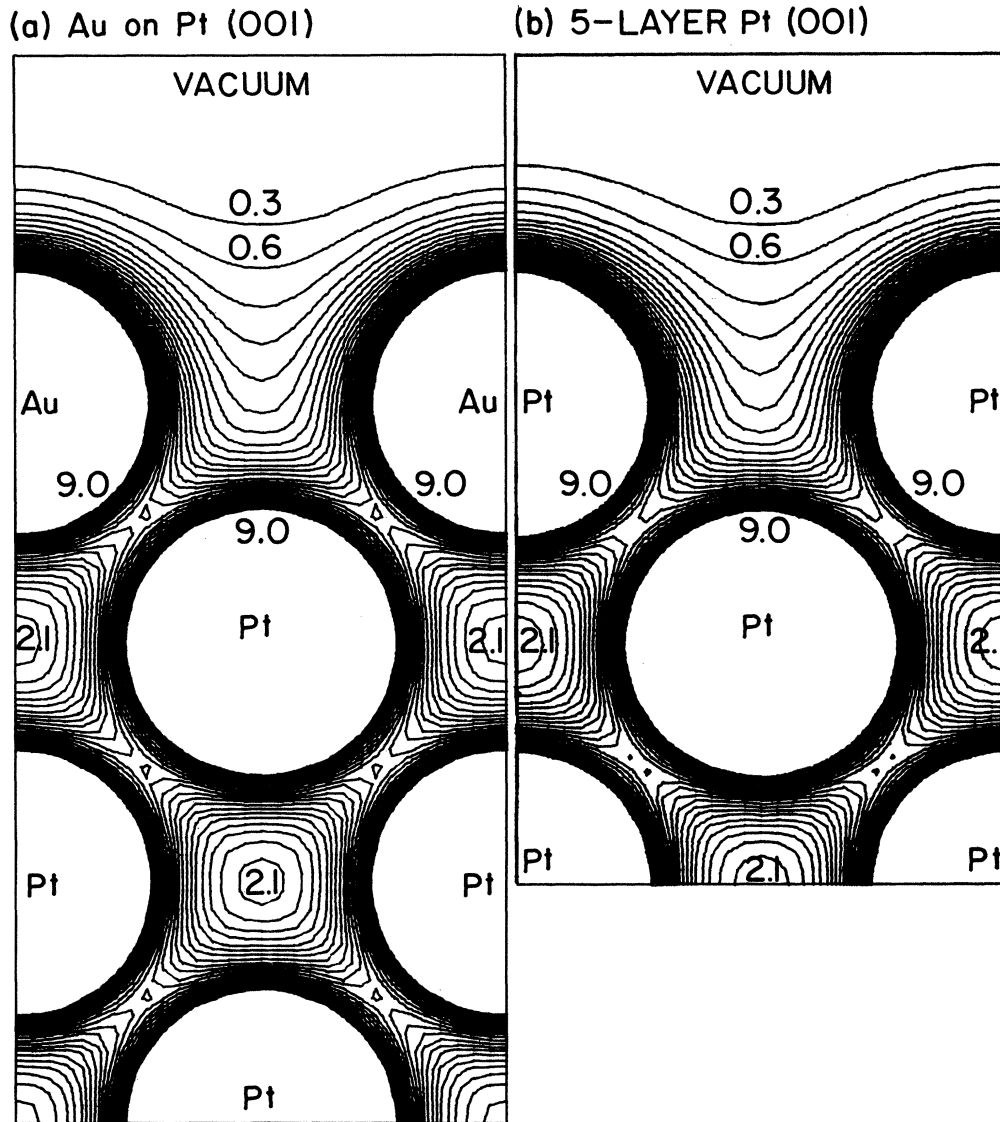


FIG. 1. Self-consistent total charge density of (a) a seven-layer film consisting of a Pt(001) five-layer substrate covered with a Au-monolayer film on each side, and (b) a clean Pt(001) five-layer film. These contour plots are shown on a vertical-cut plane passing through a line connecting a surface atom with one of its nearest neighbors in the second plane of atoms. The contour unit is 0.01 a.u.

TABLE I. Total number of valence electrons inside touching muffin-tin spheres, and their orbital decomposition for the Au/Pt film, clean Pt(001) film, and isolated Au-monolayer film. S , I , $S-1$, $I-1$, and C denote the surface, interface, subsurface, subinterface, and center layer, respectively.

	Layer	Total	s	p	d	f
Au/Pt	Au(S)	9.85	0.06	0.35	8.83	0.05
	Pt(I)	9.05	0.60	0.47	7.90	0.08
	Pt($I-1$)	9.02	0.57	0.50	7.84	0.09
	Pt(C)	9.02	0.57	0.50	7.83	0.09
Pt	Pt(S)	8.81	0.56	0.34	7.84	0.05
	Pt($S-1$)	9.00	0.57	0.50	7.81	0.09
	Pt(C)	8.98	0.58	0.50	7.78	0.09
Au	Au(S)	9.67	0.62	0.16	8.87	0.02

tal and l -decomposed number of valence electrons *inside the muffin-tin spheres* of the various slabs for which calculations were performed. The number of d -band electrons inside the interior Pt atoms is seen to be the same on both the Au/Pt and clean Pt slabs to within about 0.04 electrons. Experience has shown that the finite sampling used in performing the Brillouin-zone integrations can cause changes of this magnitude when comparing two different self-consistent calculations. The Pt(I) atom has 0.06 more electrons than the Pt($I-1$) atom, while the Pt(S) atom has only 0.03 more electrons than the Pt($S-1$) atom. There may thus be a small charge transfer onto the Pt(I) from the Au(S) atom. Note that the Au(S) atom has 0.04 fewer electrons than does the Au atom in the isolated monolayer. There is a much larger change in the p -like occupation for the Pt(I) compared to the Pt(S). This is essentially due to the reduced coordination of the surface atom, since the p -like component comes mostly from the tails of the $6s$ and $5d$ wave functions of neighboring atoms. Thus the Au atom in the isolated Au monolayer has the smallest number of p -like electrons, because it has only four nearest neighbors. Similar behavior has been seen for the clean Cu(001) surface and Cu(001) with a Ni-monolayer overlayer.²⁴

The work function, which is quite sensitive to the charge-density distribution is 6.60 and 6.17 eV for the clean Pt(001) and the Au/Pt(001) film, respectively. The experimental result is 5.7 eV for the Pt(001) film.²⁵ The difference of 0.9 eV between theory and experiment is larger than our results for the other systems studied, namely Al (Ref. 26), Cu (Ref. 24), and W.²² This may be due to the reconstruction present on the Pt(001) surface but not included in our theoretical model. The calculated decrease, 0.43 eV, of the work function after the monolayer coverage of the Au overlayer is consistent with the experimental fact that the work function of Au is 5.1 eV, about 0.6 eV less than the value for Pt. The small charge transfer from the Au(S) atom onto the Pt(I) is also consistent with the reduction in work function, since it acts to reduce the magnitude of the spillout dipole barrier.

Energy shifts of surface-atom core-level states with respect to the same atom in the interior are also sensitive to small transfer of charge and changes in the d -band electronic structure. The $4f_{7/2}$ core-state energies (with respect to the Fermi energy) for the different slabs are given in Table II. We first note that the Pt(C) and Pt($I-1$) eigenvalues on Au/Pt and clean Pt are the same to within about 0.1 eV. On the clean Pt slab, the Pt(S)

eigenvalue shifted to about 0.7 eV reduced binding energy compared to the Pt($I-1$) and Pt(C) atoms. While no measurements have been reported for Pt(001), shifts of 0.40 and 0.55 eV have been reported²⁷ for Pt(111) and Pt(110), respectively. Qualitatively, the shift to reduced binding energy is related to narrowing of the surface d band and is predicted by two somewhat disparate simple models as discussed by Feibelman.²⁸ On the Au/Pt slab, the Pt(I) $4f_{7/2}$ level is shifted to only 0.25 eV reduced binding energy, compared to the Pt($I-1$) and Pt(C) atoms. The reduction of the magnitude of the shift comes about from two competing effects: (i) the increased coordination of the Pt(S) atom on the Au/Pt slab tends to equalize its core-state energy with that of the interior atoms, while (ii) the small-charge charge transfer onto the Pt(S) atom (Table I) tends to reduce its binding energy through more effective screening of the nucleus.

The layer projected density of states (DOS) of the clean Pt(001) five-layer film is shown in Fig. 2. The top panel shows the difference between the surface layer and the average of the inner three layers. The $5d$ bands of the Pt

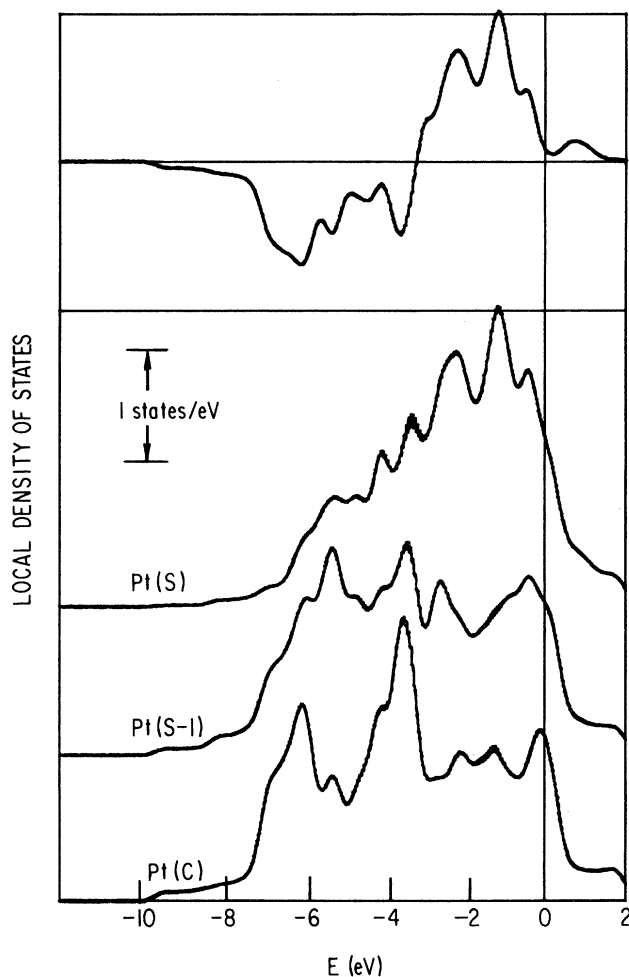


TABLE II. $4f_{7/2}$ core-level eigenvalues, the Au/Pt film, clean Pt(001) film, and isolated Au-monolayer film (in eV) with $E_F=0$. The order of the atomic layer as shown in the left column is from the center (at the bottom) to the surface.

	Au/Pt	Pt	Au
Au	-76.22		-75.61
Pt	-65.23	-64.76	
Pt	-65.50	-65.46	
Pt	-65.53	-65.63	

FIG. 2. Layer-projected DOS of a clean five-layer Pt(001) film. S , $S-1$, and C denote the surface, subsurface, and center layer, respectively. The top panel shows the difference between the surface layer and the average of the three inner layers.

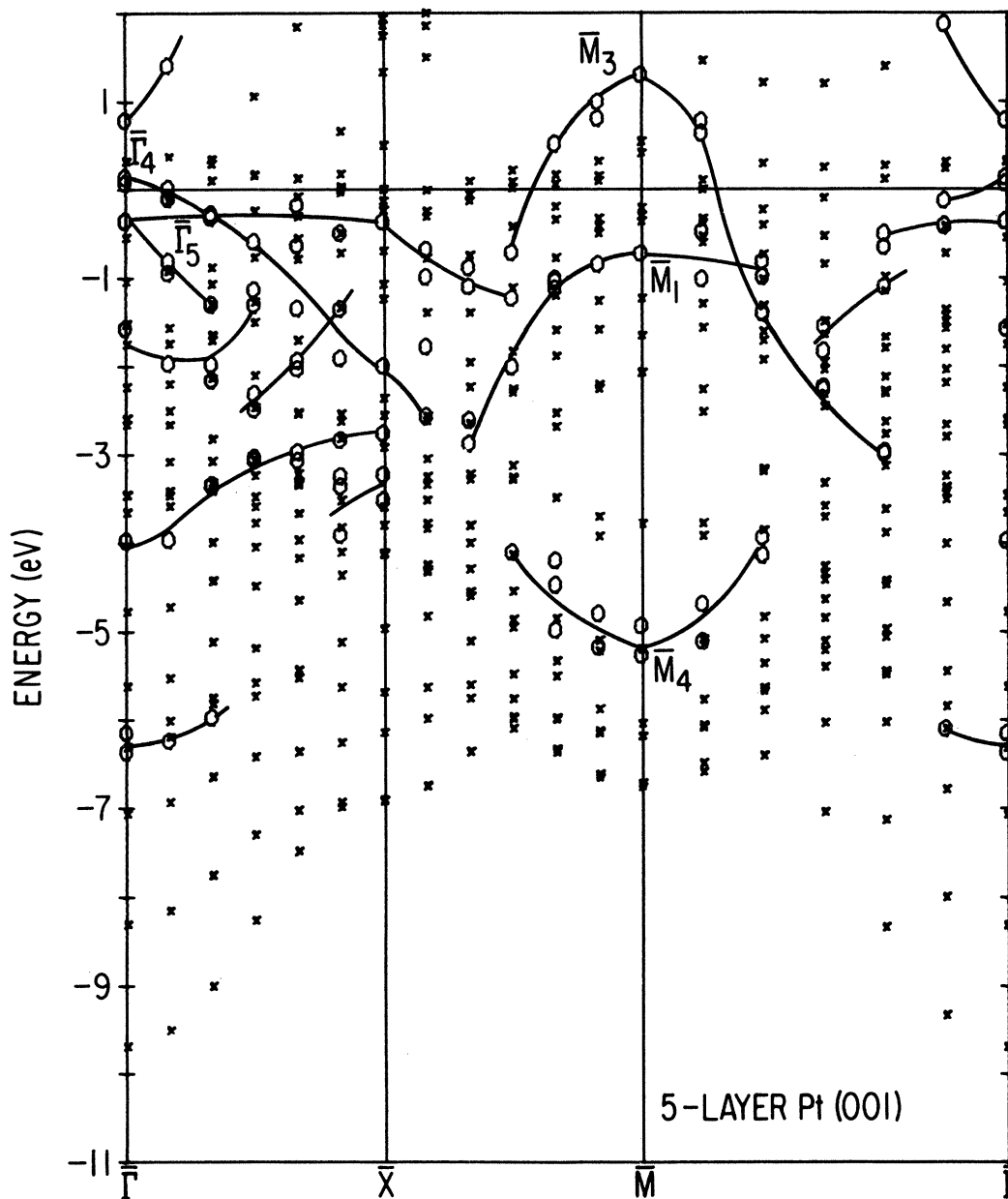


FIG. 3. Band structure of a five-layer Pt(001) film. Solid circles denote a state with more than 60% of its electrons in the surface Pt layer. Subscripts 1, 3, 4, and 5 denote $d_{3z^2-r^2}$, $d_{x^2-y^2}$, d_{xy} , and $d_{xz,yz}$ states, respectively.

center layer spread from -7.8 to 0.5 eV. The bottom of the valence band (-9.7 eV) and the DOS at E_F (20.4 states per Ry) are in good agreement with the bulk calculation.²⁹ The local DOS of the surface layer clearly shows the narrowing due to the reduced coordination of the surface atoms: The surface DOS is greatly reduced at about -6.0 eV as shown in the top panel of Fig. 2, because the contribution of the $d_{xz,yz}$ bonding states is shifted to higher energies due to the loss of the nearer neighbors above the surface.

The band structure of this Pt(001) film is plotted in Fig. 3. The solid circles denote surface states defined as states having more than 60% of their weight in the surface

layer. The notable features of Fig. 3 include the localized antibonding $d_{xz,yz}$ states around the $\bar{\Gamma}_5$ state and the antibonding $d_{3z^2-r^2}$ states around \bar{M}_1 . These bands are rather flat and quite close to the Fermi energy, so they contribute to the surface DOS and are responsible for the peak close to E_F seen in the plot of the difference of the DOS shown in the top panel of Fig. 2. Another surface band around \bar{M}_3 is lifted above the upper edge of the bulk 5d bands. This $5d_{x^2-y^2}$ state³⁰ is in the gap between the d and sp bands. A similar phenomenon has been observed for Cu,^{21,24,31,32} Ni,^{24,33-35} and the Ni overlayer on a Cu substrate.²⁴

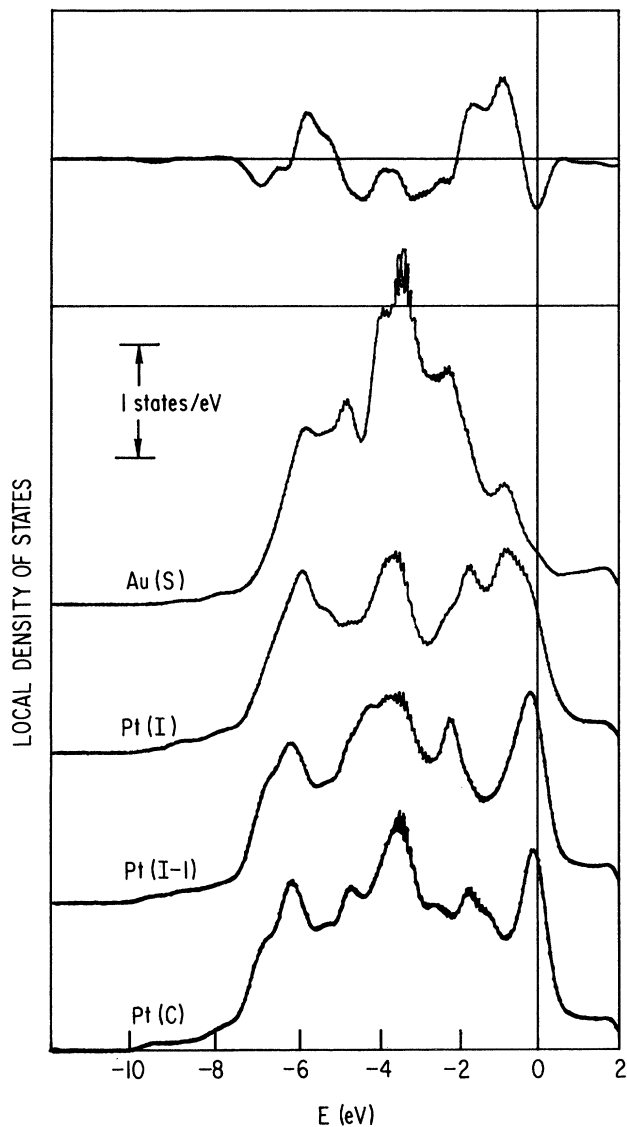


FIG. 4. Layer projected DOS of a five-layer Pt(001) slab covered with a $p(1 \times 1)$ monolayer of Au on each side. *S*, *I*, *I* - 1, and *C* denote the surface, interface, subinterface, and the center layer, respectively. The top panel shows the difference between the interface-Pt layer and the average of the three innermost Pt layers.

After coverage with a Au monolayer, the local DOS of the interface Pt layer becomes more bulklike: The surface narrowing has disappeared and its bandwidth becomes the same as that of the center layer, as is seen in the curve labeled Pt(*I*) in Fig. 4. However, as shown in the top panel of Fig. 4, the interface-Pt layer still retains the rather strong increase in the DOS from -1.8 to -0.4 eV over the center layer. Another important feature is that the Au DOS is completely filled—there are no *d* holes which could increase the reactivity of the surface. The band structure of the Au/Pt slab is plotted in Fig. 5 and may give a better understanding of this change in the Pt(*I*) layer. A monolayer coverage of an Au overlayer on the Pt leads to the delocalization of a number of the Pt surface

states existing on the clean Pt(001) surface; some of the surface states seen in Fig. 3 do not appear in Fig. 5 as interface states anymore. However, in the band plot the Pt interface bands around $\bar{\Gamma}_5$ and \bar{M}_1 are still well localized, which obviously contributes to the difference between the interface and center layers (top panel in Fig. 4). The surface Au states are connected by the solid curves in Fig. 5. The Au $d_{3z^2-r^2}$ and d_{xy} states, which are directed to the next-nearest neighbors, remain localized, but the Au $d_{xz,yz}$ and $d_{x^2-y^2}$ states mix with the substrate Pt state and do not appear as surface states in Fig. 5. The exception is at \bar{M} , where the mixing of the Au \bar{M}_3 ($d_{x^2-y^2}$) state with an *s*, *p*, or *d* state of the nearest neighbors is forbidden by symmetry, and this results in a rather well-localized surface state. Note in particular that the Au \bar{M}_3 contributes to the surface DOS at about -0.6 eV.

A plot of the isolated Au(001)-monolayer film bands (with lattice constant equal to the Pt crystal) is given in Fig. 6. Aside from the greatly reduced *d*-band width, the most notable feature is the hole pocket created at \bar{M} by the \bar{M}_3 state which has been shifted above E_F . [A similar hole pocket had been reported by Cooper³⁶ in a non-self-consistent calculation for a Cu(001) monolayer, but a later self-consistent calculation³⁷ found no *d* holes.] The presence of such *d* holes has stimulated speculations about the possibility of magnetic ordering in such a monolayer deposited on an insulating or metallic substrate. It is clear, however, from our results for the Au/Pt slab (Figs. 4 and 5), that the interaction of the monolayer with a metallic substrate greatly broadens the *d* band, and this removes the small *d*-hole pocket.

Finally, as mentioned, the DOS in the Au atomic layer in the Au/Pt slab of Fig. 4 is completely filled—the small *d*-hole pocket of the monolayer is completely removed and it is difficult to see how this Au layer could be responsible for any increase on the reactivity of the surface.

IV. CONCLUSIONS

We have presented results of all-electron self-consistent semirelativistic local-density-functional investigations of the clean and Au-covered Pt(001) surface. These studies were carried out in an attempt to shed light on experimentally observed enhanced reactivity of the Au/Pt surface. The charge density within the fourfold hollow sites at the surface was found to be very similar on both surfaces, as expected. The work function of the Au/Pt surface was reduced by 0.43 eV compared to the clean Pt surface. The interface-atom $4f_{7/2}$ core-state level on the Au/Pt surface is shifted by 0.3 eV to reduced binding energy, while the surface atom on clean Pt is shifted by 0.7 eV to reduced binding energy. On the clean Pt surface the DOS in the surface atomic layer shows a large peak at about -1.0 eV due to surface states. This peak persists at -1.0 eV after Au coverage on the Au/Pt surface and is due to a band of interface states localized on the interface Pt atomic layer. Significantly, however, there are *no* states on the Au/Pt surface which are localized both on the Au and interface-

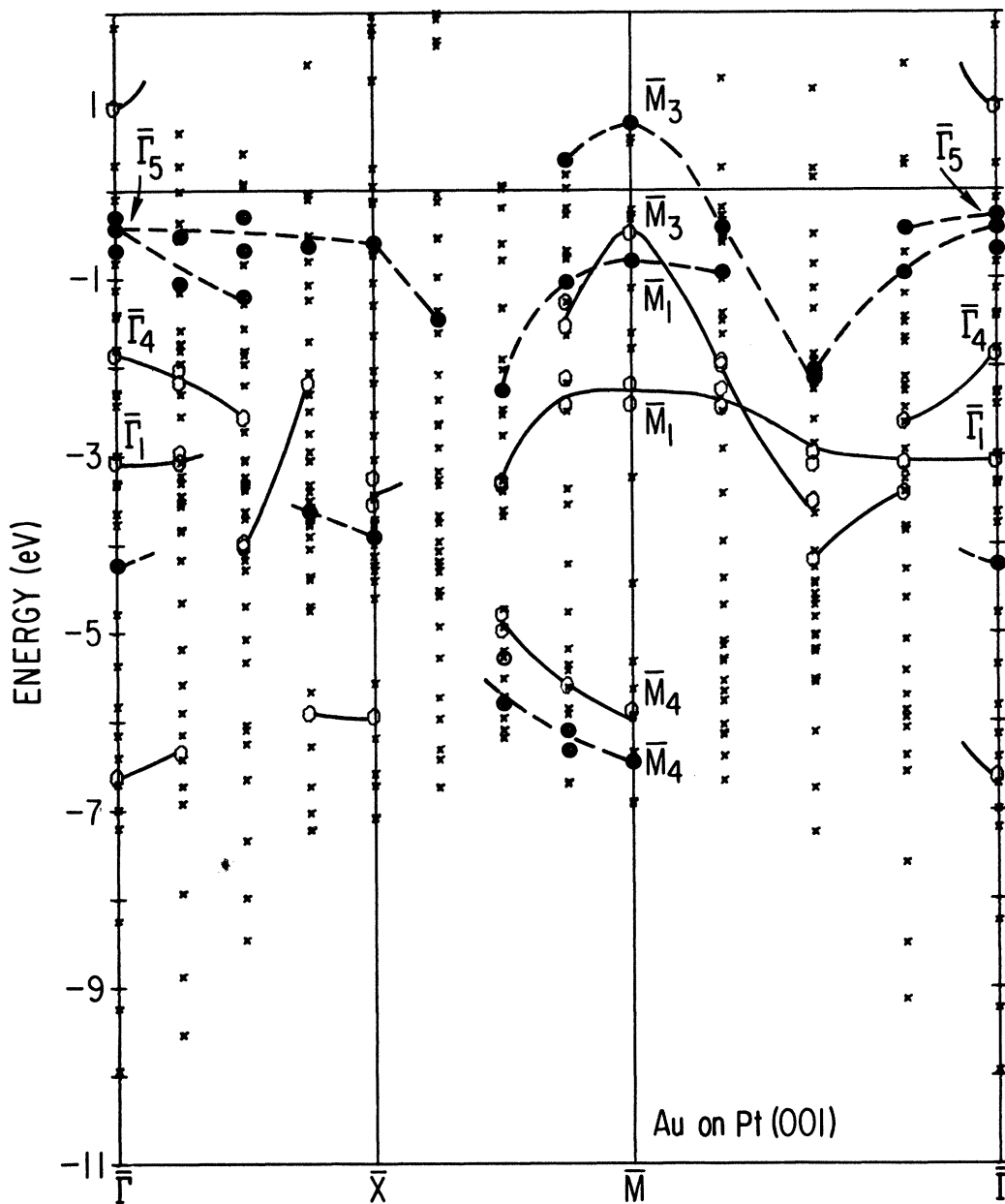


FIG. 5. Band structure of a five-layer Pt(001) slab covered with a $p(1 \times 1)$ monolayer of Au on each side. Solid circles denote states with more than 50% of their electrons in the interface-Pt layer. Open circles denote states with more than 60% of their electrons in the surface Au layer. Subscripts 1, 3, 4, and 5 denote d_{z^2} , $d_{x^2-y^2}$, d_{xy} , and $d_{xz,yz}$ states, respectively.

Pt layers. Furthermore, the d -band DOS on the adsorbed Au layer is fully occupied. Since d -band occupancy is related to chemical reactivity, the adsorbed Au monolayer probably plays no direct role in the experimentally observed enhanced reactivity—i.e., the 4% contraction of the Au monolayer does not appear to have any significant effects. Assuming that the experimentally studied surface was indeed a well-ordered Au monolayer in exact registry with the Pt substrate, it is still possible that the analytically active site is the interface-Pt atomic layer which is accessed through the fourfold hollow. The enhanced reac-

tivity might be explained by the fact that the chemically inactive Au atoms prevent the hole from being “closed” by “poisoning” with carbon atoms. This last possibility seems unlikely to us.

In view of the results of our calculations, a more reasonable conclusion is that the morphology of the experimentally observed surface was quite *different* from that modeled here. For example, sizable “patches” of the surface may have consisted of an alloylike phase of *coplanar* Au and Pt atoms. This is only one of many possible ways in which the $p(1 \times 1)$ structure of the Pt(001) surface may

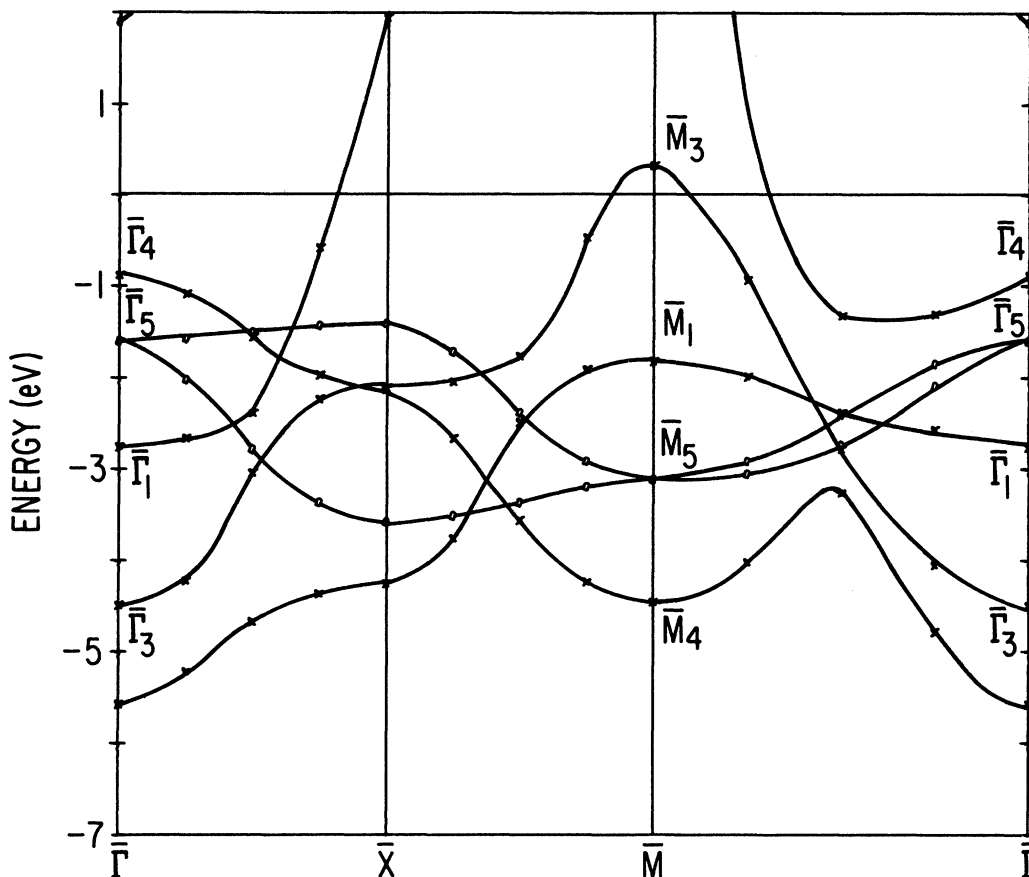


FIG. 6. Band structure of an isolated monolayer Au film (with 4% contraction with respect to bulk crystal lattice). Subscripts 1, 3, 4, and 5 denote $d_{3z^2-r^2}$, $d_{x^2-y^2}$, d_{xy} , and $d_{xz,yz}$ states, respectively.

have been disrupted by the process of Au deposition. Evidence for this has been seen in several other systems: In the case of CO on submonolayer Cu-covered Ru(001) there is evidence,³⁸ based on the nonuniform attenuation of the Cu and Ru d -band emission upon CO dosing, which suggests that chemisorption-induced segregation may play a role in uncovering Ru sites. This latter point is similar to that suggested for the Cu-Ni system.³⁹ Thus it would be very helpful if the actual surface structure could be studied during the reaction process.

ACKNOWLEDGMENTS

We are grateful to S. D. Bader for helpful discussions. Research at Northwestern University and Argonne National Laboratory was supported by the U.S. Office of Naval Research (Grant No. N00014-81-K-0438), and the U.S. Department of Energy, and by a grant from The Xerox Foundation. Research at the College of William and Mary was supported by the National Science Foundation (Grant No. DMR-81-20550).

¹T. E. Fischer, *Phys. Today* **27**, (5), 23 (1974).

²*The Physical Basis for Heterogeneous Catalysis*, edited by E. Drauglis and R. I. Jaffee (Plenum, New York, 1975).

³H. P. Bonzel, *Surf. Sci.* **68**, 236 (1977).

⁴M. Boudart, *Adv. Catal.* **20**, 153 (1969).

⁵J. H. Sinfelt, *Prog. Solid State Chem.* **10**, Part 2, 55 (1975).

⁶M. Boudart, *J. Vac. Sci. Technol.* **12**, 329 (1975).

⁷J. H. Sinfelt, *Rev. Mod. Phys.* **51**, 569 (1979).

⁸G. A. Somorjai, *Catal. Rev.* **7**, 87 (1972).

⁹J. T. Yates, T. E. Madey, and M. J. Dresser, *J. Catal.* **30**, 260 (1973).

¹⁰K. Baron, D. W. Blakely, G. A. Somorjai, *Surf. Sci.* **41**, 45 (1974).

¹¹H. Conrad, G. Ertl, J. Koch, and E. E. Latta, *Surf. Sci.* **43**, 462 (1974).

¹²K. Christmann, G. Ertl, and T. Pignet, *Surf. Sci.* **54**, 365 (1976).

¹³S. M. Davis and G. A. Somorjai, *Surf. Sci.* **91**, 73 (1980).

- ¹⁴J. W. A. Sachtler, M. A. Van Hove, J. P. Biberian, and G. A. Somorjai, *Phys. Rev. Lett.* **45**, 1601 (1980); *Surf. Sci.* **110**, 19 (1981); J. W. Sachtler, J. P. Biberian, and G. A. Somorjai, *ibid.* **110**, 43 (1981).
- ¹⁵R. K. Herz, W. D. Gillespie, E. E. Petersen, and G. A. Somorjai, *J. Catal.* **67**, 371 (1981).
- ¹⁶J. R. H. van Schaik, R. P. Dessing, and V. Ponec, *J. Catal.* **38**, 273 (1975).
- ¹⁷H. C. de Jongste, F. J. Kuijers, and V. Ponec, in *Preparation of Heterogeneous Catalysis*, edited by B. Delmon (Elsevier, Amsterdam, 1976), p. 207.
- ¹⁸V. Ponec, *Surf. Sci.* **80**, 352 (1979).
- ¹⁹J. H. Sinfelt, *Adv. Chem. Eng.* **5**, 37 (1964).
- ²⁰A. E. Morgan and G. A. Somorjai, *Surf. Sci.* **12**, 405 (1968); T. A. Clarke, R. Mason, and M. Tescari, *ibid.* **40**, 1 (1973); D. G. Fedak and N. A. Gjostein, *ibid.* **8**, 77 (1967); P. W. Palmberg and T. N. Rhodin, *Phys. Rev.* **161**, 586 (1967); J. T. Grant, *Surf. Sci.* **18**, 228 (1969).
- ²¹H. Krakauer, M. Posternak, and A. J. Freeman, *Phys. Rev. B* **19**, 1706 (1979).
- ²²M. Posternak, H. Krakauer, A. J. Freeman, and D. D. Koelling, *Phys. Rev. B* **21**, 5601 (1980).
- ²³L. Hedin and B. I. Lundqvist, *J. Phys. C* **4**, 2064 (1971).
- ²⁴D. S. Wang, A. J. Freeman, and H. Krakauer, *Phys. Rev. B* **26**, 1340 (1982).
- ²⁵H. P. Bonzel and T. E. Fischer, *Surf. Sci.* **51**, 213 (1975).
- ²⁶H. Krakauer, M. Posternak, A. J. Freeman, and D. D. Koelling, *Phys. Rev. B* **23**, 3859 (1981); D. S. Wang, A. J. Freeman, H. Krakauer, and M. Posternak, *ibid.* **23**, 1685 (1981).
- ²⁷R. C. Baetzold, G. Apai, and E. Shustorovich, *Phys. Rev. B* **26**, 4022 (1982).
- ²⁸P. J. Feibelman, *Phys. Rev. B* **27**, 2531 (1983).
- ²⁹O. K. Andersen, *Phys. Rev. B* **2**, 883 (1970).
- ³⁰In this paper, x and y are along the square edges of the 2D square lattice. They are 45° away from the cubic edges of the 3D cubic lattice, which are usually chosen as the x and y in bulk calculations, so the $d_{x^2-y^2}$ state corresponds to the d_{xy} state in the usual notation.
- ³¹J. G. Gay, J. R. Smith, and F. J. Arlinghaus, *Phys. Rev. B* **21**, 2201 (1980).
- ³²P. Heimann, J. R. Hermanson, H. Miosga, and H. Neddermeyer, *Phys. Rev. B* **20**, 3059 (1979).
- ³³C. S. Wang and A. J. Freeman, *Phys. Rev. B* **21**, 4585 (1980).
- ³⁴H. Krakauer, A. J. Freeman, and E. Wimmer (unpublished).
- ³⁵E. Wimmer, A. J. Freeman, and H. Krakauer (unpublished).
- ³⁶B. R. Cooper, *Phys. Rev. Lett.* **30**, 1316 (1973).
- ³⁷C. W. Wang and A. J. Freeman, *Phys. Rev. B* **18**, 1714 (1978).
- ³⁸S. D. Bader, L. Richter, P.-L. Cao, D. E. Ellis, and A. J. Freeman, *J. Vac. Sci. Technol. A* **1**(2), 1185 (1983).
- ³⁹D. T. Ling, I. Lindau, J. N. Miller, and W. E. Spicer, in *Applied Surface Analysis, ASTM STP 699*, edited by T. L. Bair and L. E. Davis (ASTM, Philadelphia, 1980), p. 66.